Photothermal Expansion of Droplets in Emulsions Detected by the Transient Grating Method

Kazunari Tanzawa, Noboru Hirota, and Masahide Terazima*

Department of Chemistry, Graduate School of Science, Kyoto University, Kyoto 606

(Received May 26, 1997)

A nonlinear optical effect due to the thermal energy after the photoexcitation of a light-absorbing chromophore or a metal ion contained in micro droplets (oil in water (O/W) and water in oil (W/O)) was investigated by the time-resolved transient grating method. The temporal profiles of the diffusive components of the thermal grating signals are very different from that observed in a homogeneous solution, and also depend on the emulsion systems. The profiles were consistently analyzed in terms of the droplet heating, thermal expansion, and subsequent cooling process. The size of the droplets determined from this analysis agrees with that from the dynamic light scattering method.

Heterogeneous systems of emulsions are very important and interesting for many practical applications as well as in fundamental science. For example, large optical nonlinearities from these dispersed systems have attracted much attention in optical technology.[1,2] These emulsion systems will provide a unique environment for the chemical reactions or physical properties of matter. However, experimental techniques which can detect the chemical or energetic dynamics in an inhomogeneous system are rather limited. For example, although the transient grating (TG) technique is a powerful method for studying the dynamics in a variety of phases,[3—9] most TG studies so far have been conducted in homogeneous systems. The character of the TG signal from an inhomogeneous system has not yet been explored. How shall we analyze or interpret the temporal profile from inhomogeneous systems? In this study, we aimed to clarify the temporal development of the TG signal, which is thermally induced after the photoexcitation of a dye chromophore or a metal ion in O/W (oil in water) and W/O (water in oil) emulsion systems. In particular, we focused our attention on the diffusive thermal grating (DTG) signals. This investigation on a typical TG signal from the emulsion system will be a basis for further investigations on the energetic dynamics of molecules embedded in the droplets of an emulsion.

Phenomenologically, the TG method can be explained in terms of the light-induced grating as follows.[3,4] When two pump beams are crossed in a sample, an optical interference pattern is created. The interference pattern can be written as

$$I(x,t) = I_0\{1+\cos(qx)\}, \tag{1}$$

where I_0 is the light intensity of the excitation beam and q is the grating vector. The fringe spacing of the pattern (Λ) is expressed as

$$\Lambda = \lambda/2\sin(\theta/2),$$

where λ is the wavelength of the excitation beam, and θ is the crossing angle of the two excitation beams. Owing to photoexcitation by the spatially modulated light intensity, the concentration of the excited state is modulated. The excess energy is released as heat by nonradiative deactivation of the excited states, which induces a modulation of the temperature. This periodic heating launches an acoustic wave. When a probe beam is brought into the crossing region under the Bragg condition, the probe light is diffracted (the TG signal). The grating signal due to an acoustic wave (I_{ac}) may be expressed by

$$I_{ac}(t) = I_{ac}^0\{1-\cos vqt\}^2, \tag{2}$$

where I_{ac}^0 is a constant and v is the speed of sound in the medium. After the acoustic wave passes over the monitoring region or it is completely dampened, the diffusive component of the temperature modulation remains. Since the refractive index of a material is a function of the temperature, the temperature modulation leads to a diffusive component of the thermal grating (DTG) signal. The DTG signal decays with a time constant of the thermal conduction between the grating fringes,

$$I_{TG}(t) = \alpha\{\delta n_{th}^0 \exp(-D_{th}q^2t)\}^2, \tag{3}$$

where α is a constant, δn_{th}^0 is the refractive index change due to the thermal effect and D_{th} is the thermal diffusion constant.

Several colloidal systems have been studied so far by the TG technique. These include colloidal gold,[10] carbon suspension,[11] magnetic colloid,[12] and water in oil (W/O) micelles.[13] In the colloidal gold system, about a 30 ps delay time for acoustic formation was observed and the delay was interpreted in terms of a slow nonradiative relaxation of the excited metal particles.[10] A strong TG signal from a light-absorbing colloidal suspension (carbon suspension) was reported under a strong excitation condition; the origin was attributed to vapor bubbles around carbon particles created

by strong heating of the particle.[11] Photoacoustic waves generated by the photoexcitation of reverse micelles with 2.5 and 17 nm radii were reported by Cao et al.[13] While the acoustic signal from the micelles of 2.5 nm radius appears in a similar manner to that from a homogeneous solution, the signal from the micelles of 17 nm radius showed a slow rising component in the acoustic signal. They explained the difference in terms of slow heat releasing from the interior of the micelles to the solvent. They calculated the time profiles of the acoustic waves using the thermal properties and the micelle size as a parameter, and found that the micelle sizes determined from the acoustic pattern show a reasonable agreement with those estimated from the molar ratios of water to surfactant.

Compared with these studies, which are mostly limited in the pico—nanosecond range, we studied the temporal profiles of the DTG signals observed after the photoexcitation of O/W and W/O emulsions in the nano- to microsecond range for the first time. This DTG signal has been demonstrated to be very useful for elucidating various photophysical and photochemical processes from the excited states in a number of studies.[3,5,7–9] When dye molecules in a homogeneous solution are excited, and the heat releasing is sufficiently fast, the DTG signal rises with the rate of the decay of the acoustic signal, and decays single exponentially with a rate constant of $2D_{th}q^2$ (Eq. 3). Contrary to this familiar behavior, the signal from the O/W emulsion shows a fast rise and a faster decay than $2D_{th}q^2$. The signal from the W/O emulsion shows fast and slow rises and decays with a rate constant of close to $2D_{th}q^2$, even though the heat releasing process is impulsive. These different features are successfully explained by a droplet heating model which includes different thermal expansion coefficients between water and oil (*p*-xylene). The sizes of the particles are estimated from the temporal behavior, and are compared with the size distribution obtained by the dynamic light scattering (DLS) method. Furthermore, a unique acoustic pattern is observed in this system, the origin of which is discussed. In the W/O emulsion case, the DTG signal indicates the presence of small micelles, which cannot be detected by the DLS technique, besides larger droplets. This DTG method can be a simple and sensitive method for evaluating of the size of emulsion droplets as well as for elucidating the photophysical and photochemical behaviors of molecules in heterogeneous systems.

Experimental

The experimental setup for the TG measurement has been reported previously.[7–9] Briefly, an appropriate wavelength of the grating light was selected, depending on the absorption band of the chromophores in the emulsion systems. For the O/W emulsion study, β-carotene was used as a light-absorbing molecule which can be dissolved only in the oil phase (*p*-xylene). The grating light at 463 nm from an OPO system (Spectra Physics MOPO-710) was used. For the W/O emulsion measurement, $CoCl_2$ was used as a probe to deposit the thermal energy in the system. To excite this ion, the second harmonics of a Nd–YAG laser (Spectra Physics GCR-170-10) was used for this W/O emulsion. The time profile of the grating amplitude was monitored with a He–Ne laser (Spectra Physics 155). The TG signal which passed through a glass filter (Toshiba R-60) was detected by a photomultiplier (Hamamatsu R-923) and fed into an oscilloscope (Tektronix TDS-520, 2430A). The data were transferred to a computer and averaged about 300 times. In order to prevent any incoherent light scattering from the sample solution, a cell of 3 mm optical path length and another of 1 mm path length were used for O/W and W/O emulsion, respectively. All samples were flowed during the measurement.

For the dynamic light-scattering experiment, a light beam from the He–Ne laser was brought into the sample (optical path length=1 cm) and the scattered light which passed through two pinholes was detected by a photodetector (Hamamatsu R2949) at a scattering angle of 90° under a photon counting condition. The autocorrelation of the output signal was taken by a correlator (Ohtsuka Electronics LS-7).

The sample of the O/W emulsion was prepared by the following method. A β-carotene / *p*-xylene saturated solution (0.1 ml) was dropped into 5 ml sodium lauryl sulfate (SDS) aqueous solution (1.7×10^{-1} M) (1 M =1 mol dm^{-3}) and mixed by an ultrasonic cleaner for 30 s. Into that solution, 1-hexanol (0.05 ml) was dropped, and further mixing was carried out for 30 min. After a while, the sample was separated into two layers. The lower layer, which contained oil droplets, was used for the measurement. For preparing the W/O emulsion,[14] Aerosol-OT (AOT) (60 mg) was dissolved in toluene (5.0 ml), and a saturated $CoCl_2$ aqueous solution (0.05 ml) was dropped into it. It was mixed for 30 min. *p*-Xylene was purchased from Wako Chemical Co., and all other reagents were purchased from Nacalai Tesque, Inc. All reagents were used without further purification. All measurements were carried out within several hours after the sample preparation.

Results

O/W Emulsion. Before showing the DTG signal from the emulsion solution, the time dependence of the DTG signal after photoexcitation of a dye in a homogeneous solution (Methyl Red in benzene) is depicted in Fig. 1a. Since the deactivation of Methyl Red is sufficiently faster than the pulse width (ca. 15 ns) of the excitation beam, and the width is longer than the period of the acoustic oscillation ($(vq)^{-1}$) under this condition, the acoustic wave is smeared out and only the DTG signal appears with an instrument response time. The thermal grating signal decays single exponentially with a rate constant of $2D_{th}q^2$. (In the enlarged time scale (Fig. 1a), the decay looks linear.)

The time dependence of the TG signal after the photoexcitation of β-carotene in the O/W emulsion at $q = 1.0\times10^6$ m^{-1} is shown in Fig. 1b. The signal rises completely within the excitation laser pulse followed by a very rapid decay to ca. 1/5 of the peak intensity within 30 ns after the excitation. The residual signal gradually decays to the baseline in a 200 ns time scale. A thermal grating signal that decays with a rate constant of $2D_{th}q^2$ could not be observed. These features do not depend on the laser power, the sample flow rate or the fringe spacing (Λ). However, the relative intensity of the slower decay component on the order of tens of ns varies depending on these conditions. When the power of the excitation beam was weakened, the relative intensity of the slower decay component was weakened. When the fringe spacing (Λ) became longer, the slower decay component decayed slower. When the sample flow rate was faster, the

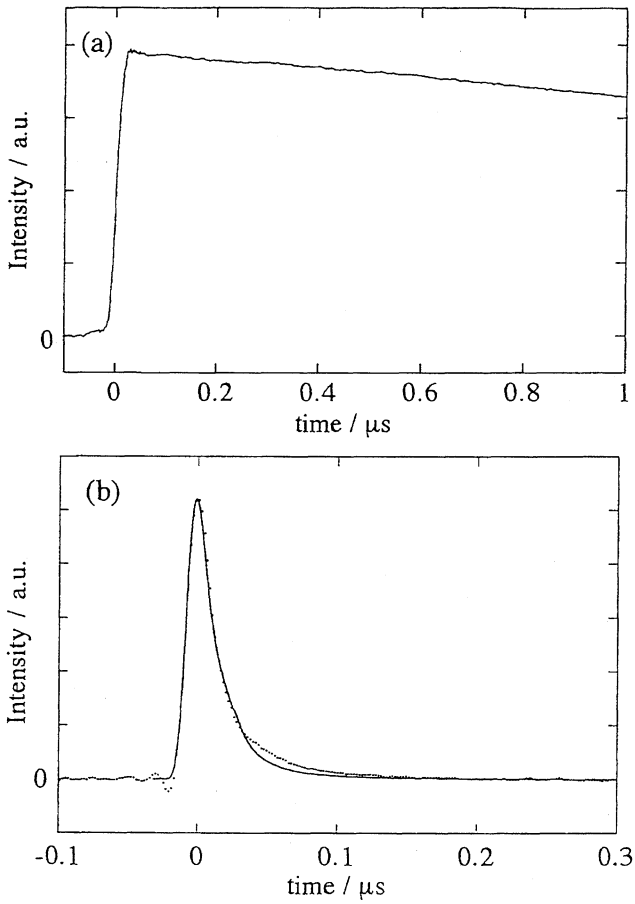

Fig. 1. (a) Temporal profile of the thermal grating signal observed after the photoexcitation of Methyl Red/benzene solution (excitation wavelength is 355 nm). (b) Temporal profile of the TG signal after the photoexcitation of β-carotene in the O/W emulsion at 463 nm (dotted line) and calculated signal from the thermal diffusion equation from a spherical particle (solid line). The weak negative peak negative peak at $t<0$ is due to electric noise from the laser.

intensity of the TG signal became stronger, and especially the rapid decay component became dominant compared with the slower decay component (Fig. 2). These tendencies imply that the origin of the slower decay component is different from that of the main part of the signal.

In order to examine acoustic waves from the emulsion system, the TG signals at a small crossing angle between the grating beams were measured ($q=7.5\times10^4$ m^{-1}). In this case, the fringe length was long enough to observe the acoustic TG signal. From a homogeneous solution, a periodic acoustic wave was clearly observed (Fig. 3a). This wave can be explained well by expression, Eq. 2. However, the feature of the TG signal from the emulsion system was very different from that typical feature (Fig. 3b). The signal consists of two peaks during one cycle of the acoustic wave from the homogeneous solution. They gradually merge, and after 400 ns from the excitation, they look like almost one peak per cycle. Besides the apparent oscillation, there is another bump (or background) signal at around 0—600 ns. This signal gradually rises, and then decays to the baseline

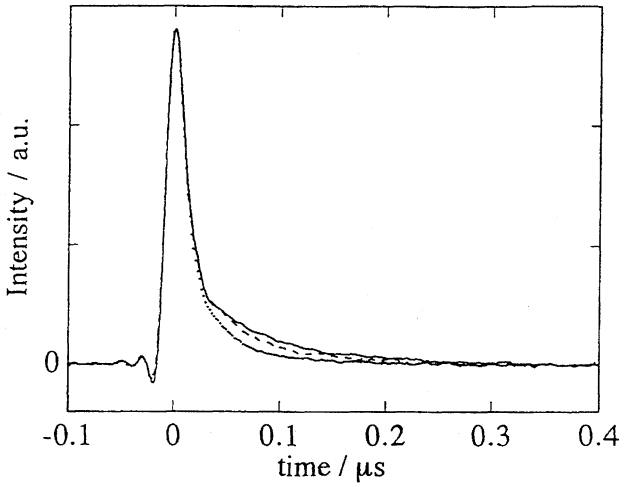

Fig. 2. The sample flow rate dependence of the TG signal from the O/W emulsion. Signals are normalized at the peak intensity. The sample flow rates are 1 cm^3 min^{-1} (solid line), 4 cm^3 min^{-1} (broken line), and 6 cm^3 min^{-1} (dotted line). The weak negative peak at $t<0$ is due to electric noise from the laser.

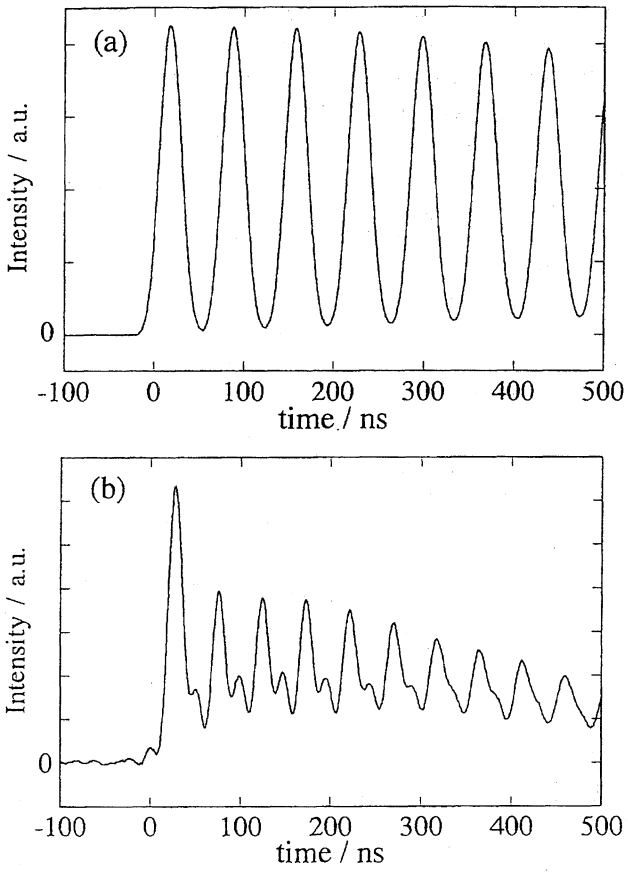

Fig. 3. (a) Temporal profile of the acoustic TG signal from Methyl Red/benzene solution. (b) Temporal profile of the acoustic TG signal from the O/W emulsion.

in about 700 ns.

The size distribution of the emulsion droplet measured by the DLS method is shown in Fig. 4.

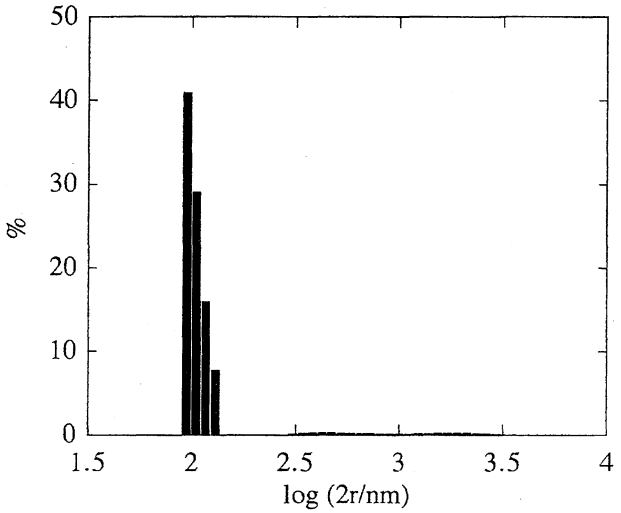

Fig. 4. The size distribution of the O/W emulsion droplets measured by the dynamic light scattering method.

W/O Emulsion. The time dependence of the DTG signal from the W/O emulsion is totally different from the O/W emulsion, and is depicted in Fig. 5. The DTG signal first rises very rapidly within the excitation pulse width and there appears a slow rising component. The signal decays to the baseline with a lifetime of 9 μs. Under the same condition, the thermal grating signal from the homogeneous toluene solution rises quite rapidly and decays with a lifetime of 10 μs.

The shorter lifetime of the DTG signal from the emulsion system (9 μs) than that from the homogeneous solution (10 μs) is beyond the experimental uncertainly. One might think that the enhancement can be explained by the larger thermal conductivity of water (1.4×10^{-7} m^2 s^{-1}) than that of toluene (9.5×10^{-8} m^2 s^{-1}). Estimating the thermal conductivity of the emulsion system from the Maxwell relation,[15—17]

$$K_E = K_c\left[\frac{K_D + 2K_C - 2\phi_D(K_C - K_D)}{K_D + 2K_C + 2\phi_D(K_C - K_D)}\right].$$

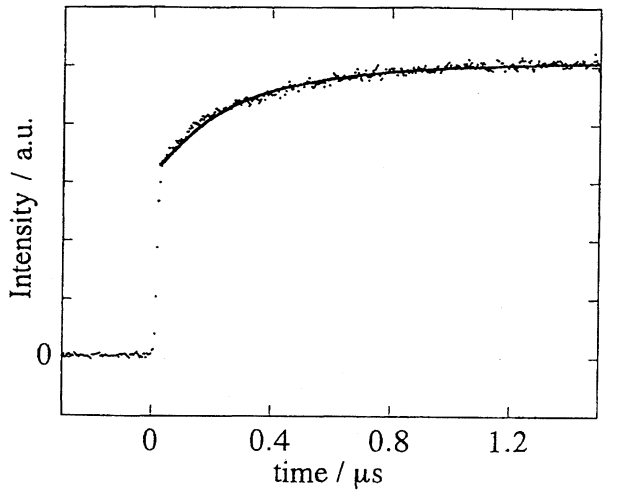

Fig. 5. The time dependence of the TG signal from W/O emulsion (dotted line) and calculated signal with the thermal diffusion equation (solid line).

(K_E, K_C, and K_D, are the effective thermal conductivity of the emulsion, the dispersing droplet, and the dispersed medium, respectively, and ϕ_D represents the volume fraction of the dispersion), we find that the effect of water on the thermal conduction is negligible in our sample. This enhanced thermal conduction was observed in other heterogeneous systems in our laboratory, and will be discussed in a separate report.

The size distribution of this emulsion droplet measured by the DLS method is shown in Fig. 6. This emulsion system has a rather broad distribution.

Discussion

After the photoexcitation of β-carotene or Co^{2+}, electronic excited states are created. Since the nonradiative relaxation processes of these excited states of β-carotene and Co^{2+} are fast,[18—20] the observed TG signal should come from the thermal contribution of the nonradiative transition (not the population grating). The observed TG signal from the O/W and W/O emulsion systems can be interpreted as follows.

O/W Emulsion. In order to explain the temporal profile of the DTG signal, which is quite different from that obtained from a homogeneous solution, the local heating of the droplets is considered. First, only the emulsion droplets should be heated by the deactivation from the excited states of the probe molecule, which is embedded in the droplet. Due to the temperature rise, the volume of the oil droplet will expand. The expansion causes a decrease of the density and the refractive index; this change should be detected as the TG signal. As time goes on, the thermal energy flows out from the droplets to the environment by the thermal conduction, and the droplet contracts. Together with the signal disappearance due to this contraction, the thermal energy in the medium results in elevating the temperature of water, and the thermal grating signal due to the density modulation of the water phase should be observed. However, since the thermal expansion coefficient and the molecular polarizability of water are much smaller than those of xylene, the TG

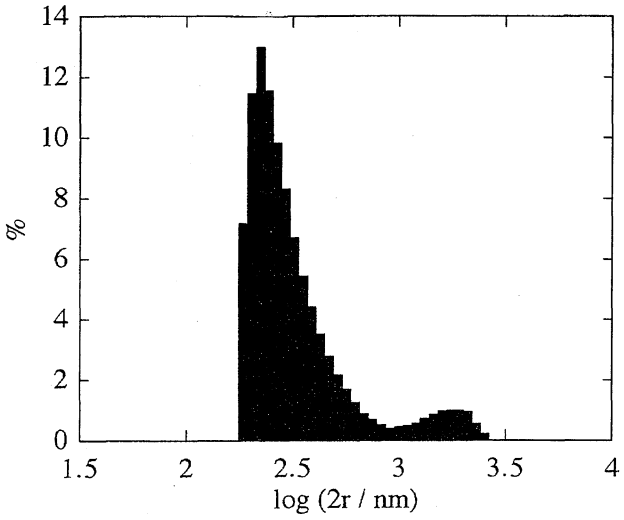

Fig. 6. The size distribution of the W/O emulsion droplets measured by the dynamic light scattering method.

signal due to the thermal expansion of the droplet is expected to be much stronger than that due to the thermal expansion of medium (water). Therefore, the first appearing TG signal is assigned to a signal by the local density grating, and the fast decay is attributed to the thermal conduction from the droplets to water. The basic idea of this local heating model is the same as that of a model which was used to explain the temporal behavior of acoustic waves from reverse micelle solutions by Diebold and co-workers.[13]

We tried to reproduce the observed TG profile based on this model. Since the dominant contribution to the DTG signal comes from the density change by the thermal effect, and the size of the dorplets is sufficiently smaller than the fringe spacing ($\Lambda = 6$ μm), the DTG intensity should be calculated from the refractive index change due to the volume expansion of the system. First, the volume changes of the oil phase and the water phase are calculated from the specific heats and thermal expansion coefficients of *p*-xylene and water.[21,22] The refractive index change accompanied by the volume expansion is then calculated from the Lorenz–Lorentz relation, which is given by,

$$\frac{n^2-1}{n^2+2} = \frac{1}{3\varepsilon_0} N\alpha, \tag{4}$$

where α is the molecular polarizability and N is the number density of molecules.[21,22] From these quantities, the ratio of the TG signal intensity from the droplet density change to that from the solven's dnsity change is estimated to be about 20000 : 1. Because of this large difference, the slovent's density grating component is not observed, as shown in Fig. 1b.

The time dependence of the TG signal should be reproduced by that of the refractive index change based on this model. The time dependence of the droplet's temperature can be calculated from the thermal diffusion equation. The diffusion equation in three dimensions with a spherical heat source (r; radius) is expressed by[23]

$$\frac{\partial u}{\partial t} = D_{\text{th}} \frac{\partial^2 u}{\partial^2 r}, \quad r > 0. \tag{5}$$

Here, $u = \Delta T \cdot r$ (ΔT: temperature rise) and for the sake of simplicity, the thermal diffusion constants of xylene and water are assumed to be equal ($D_{\text{th}} = 1.4\times10^{-7}$ m^2 s^{-1}). We further assume that the temperature of the droplet rises uniformly at $t = 0$. This assumption seems to be reasonable because of the small absorbance ($A \approx 0.5$) and small size of the droplets (ca. 100 nm as shown later) compared with the excitation wavelength. Taking the radius of the sphere to be a, and the initial temperature in the sphere $0<r<a$, ΔT_0, the initial condition is given by

$$\begin{aligned} u &= \Delta T_0 \cdot r, && \text{when } t = 0,\ 0 < r < a, \\ u &= 0, && \text{when } t = 0,\ r > a, \\ u &= 0, && \text{when } r = 0. \end{aligned}$$

The analytical solution is expressed by[23,24]

$$\Delta T(r,t) = \frac{1}{2}\Delta T_0 \left\{ \operatorname{erf}\frac{(a-r)}{2\sqrt{D_{\text{th}}t}} + \operatorname{erf}\frac{(a+r)}{2\sqrt{D_{\text{th}}t}} \right\}$$

$$-\frac{1}{r}\sqrt{\frac{D_{\text{th}}t}{\pi}} \left\{ \exp\frac{-(a-r)^2}{4D_{\text{th}}t} - \exp\frac{-(a+r)^2}{4D_{\text{th}}t} \right\}. \tag{6}$$

We define the reduced radius (r') by

$$r' = \frac{r}{a}. \tag{7}$$

The time dependence of the averaged sphere's temperature ($\Delta\overline{T}(t)$) is obtained by integrating the equation from $r' = 0$ to 1. (This corresponds to the integration over the inside of the sphere.)

$$\Delta\overline{T}(t) = \int_0^1 4\pi r'^2 \Delta T_0 \left[\frac{1}{2} \left\{ \operatorname{erf}\frac{(1-r')}{2\sqrt{b}} + \operatorname{erf}\frac{(1+r')}{2\sqrt{b}} \right\} \right.$$

$$\left. -\frac{1}{r'}\sqrt{\frac{b}{\pi}} \left\{ \exp\frac{-(1-r')^2}{4b} - \exp\frac{-(1+r')^2}{4b} \right\} \right] \mathrm{d}r', \tag{8}$$

where

$$b = \left(\sqrt{\frac{D_{\text{th}}t}{a^2}} \right)^2. \tag{9}$$

In this calculation, we assume that the volume change is so small that the droplet radius is constant. When the temperature change is small, the refractive index change due to the density change is proportional to the temperature rise. In order to fit the TG data with this calculation, the time profile of δn_{th} is convoluted with the excitation laser pulse and then squared. The adjustable parameter in the fitting is only the radius of the droplet. The agreement is quite good, as shown in Fig. 1b. The droplet size obtained from the fitting is 1.1×10^2 nm. The calculated profile slightly disagrees with the experimental data in the 30—150 ns range. As stated in the previous section, in this time range we observed a weak bump, whose shape depends on q, the sample flow rate, and the laser power. Therefore, we think that this bump signal cannot be explained by this local-heating model, but comes from a different mechanism, which we do not completely understand. In the above fitting process, we tried to use the calculated curve to reproduce the observed signal in a fast time scale.

As shown in Fig. 4, the droplet size measured by the DLS method has a sharp peak at 100 nm. The droplet size of the main peak agrees well with the size determined from an analysis of the TG signal (1.1×10^2 nm).

Finally, in this section, we comment on the acoustic waves observed from the O/W emulsion. The observed double-frequency oscillation cannot be explained in terms of the ordinary periodic density expansion due to the thermal effect. Indeed, acoustic waves after the photoexcitation of W/O emulsion reported previously did not show any higher harmonic component.[13] Electrostriction will produce an overtone of the oscillation.[25] However, since the acoustic signal was not observed without the light-absorbing molecule, the signal cannot be due to the effect of the electrostriction. Essentially, the acoustic signal should be explained by a similar model as that for the DTG signal. As discussed above, the temporal profile of the DTG signal indicates droplet expansion followed by a gradual contraction. Based on this

model, we may describe this pressure wave qualitatively as follows. At first, a pressure wave is launched by expansion of the droplets; then, a 'negative (or reverse)' pressure wave is created by a contraction process which is associated with thermal cooling. Since these processes are temporally shifted relative to each other, they do not completely cancel, and produces compressed-sparse waves. This produces an overtone signal of the acoustic signal, because the TG signal intensity is proportional to the square of the density change. Interestingly, a very similar acoustic wave was observed after strong photoexcitation of a carbon suspension by Chen and Diebold.[26] They explained the temporal behavior in terms of the density wave induced by a photochemical reaction.

The time dependence of the density change after a thermal expansion and a molecular volume change can be calculated by solving the linearized hydrodynamic equation with molecular volume changes. Here, for simplicity, we assume that the droplet expansion occurs immediately after excitation, and that the contraction process can be expressed by a single exponential. Under the condition that the acoustic damping and thermal diffusion time can be neglected, and that the stored energy in the excited state is negligible, the density variation ($\delta\rho$) may be given by[27]

$$\delta\rho \propto \frac{\alpha E_0 \beta}{C_p}(\cos vqt - 1) + \rho N \beta_c \left\{ \frac{-e^{-\hat{k}vqt} + \cos vqt - \hat{k}\sin vqt}{1+\hat{k}^2} \right\}, \quad (10)$$

where E_0 is the fluence of the excitation light, α the absorption coefficient, C_p the heat capacity under constant pressure, N the concentration of a droplet excited by the excitation light, β the thermal expansion coefficient, β_c the chemical expansion coefficient (or, in this case, the droplet expansion coefficient), ρ the density, and $\hat{k}$ a dimensionless rate of the droplet contraction ($\hat{k}=k/vq$ and k; rate of the contraction). The first term in Eq. 10 describes the time dependence of the thermally generated acoustic wave; it is the second term that is caused by a volume expansion of the droplets. Typical temporal profiles of these terms are depicted in Fig. 7.

If the interpretation of the DTG signal is exactly applicable to this acoustic signal, the thermal expansion of the dispersed medium can be neglected. Under this condition, the observed acoustic signal should be described solely by the second terms of Eq. 10. Although the overtone oscillation is reproduced only from the second term (Fig. 7), the calculated TG signal is very different from the observed signal regarding the overall feature. If the contributions from the first and second terms are considered to be the source of the TG signal, the calculated signal becomes closer to the observed one, and the essential features, the stronger first peak intensity compared with the other ones and the overtone component, can be reproduced using an appropriate weight factor for both contributions.

Some differences, however, are still notable. One of the main differences between the calculated and observed signals is the position of the peak of the overtone oscillation. The peak of the overtone oscillation seems to be shifted to an early time from the valley of the fundamental oscillation, which

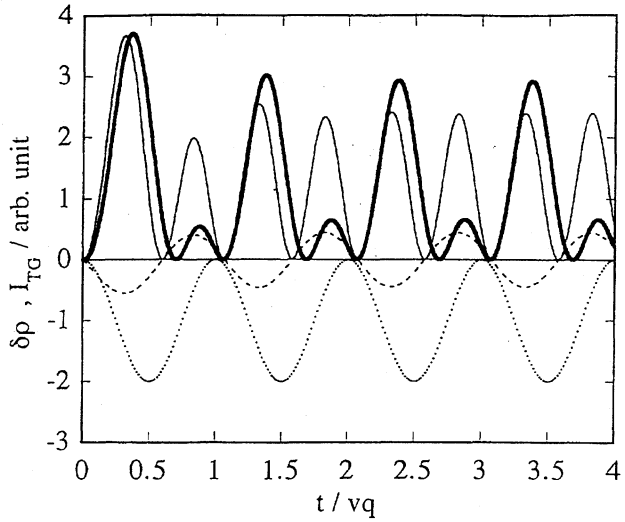

Fig. 7. Density variation $\delta\rho$ after droplet expansion calculated with Eq. 10. The dotted and broken lines represent the contributions from the first and the second terms in Eq. 10, respectively. Expected TG signal only from the second term is shown by the thinner solid line ($\hat{k}$=2) and the TG signal from the first and the second terms is shown by the thicker line ($\hat{k}$=2, and $\frac{\rho N \beta_c C_p}{\alpha E_0 \beta}$=5).

cannot be reproduced. This difference might be explained by considering the absorptive contribution in the TG signal. This point will be discussed in the future.

W/O Emulsion. The TG time profile observed from the W/O emulsion sample can be explained by the same model as in the O/W case. Only water droplets are heated after photoexcitation. After that, the thermal energy is diffused out from the droplets to the oil matrix. The difference from the O/W case is that the thermal expansion coefficient of a droplet (water) is much smaller than that of the dispersion medium. Therefore, the TG signal just after heating of the droplet is much weaker than the signal after the thermal energy is transferred to the medium. This will cause a slowly rising component, which reflects the solvent expansion process due to the thermal diffusion from the droplet. Previously, the acoustic signal after photoexcitation of reverse micelles was explained based on this model.[6]

If this model is appropriate for the DTG signal, we should be able to calculate the relative intensity ratio of the fast and slow rising components by the same method as described in the previous section. Calculating Δn with the thermodynamical parameters, one will find that the intensity of the fast rising component should be as weak as 1/120 of the slow rising component. However, the observed difference in the intensity is not so large, as shown in Fig. 5. The disagreement between the experimental and calculated values may be explained by the presence of ions embedded in much smaller water droplets or micelles without water. In order to examine this possibility, we measured the TG signal after removing water droplets from the emulsion. The droplets were removed by filtering the emulsion with a hydrophobic membrane (Sartorius Minisart SRP 15 pore size 0.2 μm). By

this procedure, we obtained a completely transparent solution, which indicates that the droplets of an emulsion size larger than sub-micrometer are removed. However, a strong TG signal that rises within the laser pulse width is observed from the solution. This fact indicates that Co^{2+} is contained in very small water droplets or micelles, from which the thermal energy is diffused out within the excitation laser pulse width. Considering the electric charge of Co^{2+}, it cannot be dissolved in toluene directly. Probably AOT makes very small micelles without water or with a small amount of water. (We may call this ion the ion in the dispersion phase, although it could not be rigorously true.) The radius of AOT-micelle is reported to be on the nm-order,[14] and the thermal diffusion from the micelle should be on the 0.1 ns order. This time delay should be detectable on a faster time scale, as Cao et al. have demonstrated using the acoustic wave.[13]

The heat flowed from inside to outside of the droplet is calculated with the equation described in the previous section. From the calculated time profile of the temperature rise of the oil matrix (D_{th}=9.5×10^{-8} m^2 s^{-1}), the slow rise profile of the TG signal can be estimated. By a superposition of thus-calculated signal and the thermal grating signal from the ions in the dispersion matrix (which should give the fast rise within the laser pulse and decays single exponentially), the observed signal can be reproduced well, as shown in Fig. 5. The adjustable parameter for the fitting is the radius of the water droplet and the relative amount of Co^{2+} in the water droplets and in the dispersion medium. From the fitting, the diameter of the droplet is determined to be 534 nm and the ratio of [Co^{2+}] in the water droplet to that in the dispersion medium is about 1 : 210.

As shown in Fig. 6, the distribution of the droplet size determined from the DLS method has a peak at about 230 nm and a broad bandwidth. The disagreement between both measurements may come from the averaging effect of this broad distribution. If we take into account the size distribution in the curve-fitting process of the DTG signal, we should be able to determine the size distribution as well.

Conclusion

The TG signals after the photoexcitation of light-absorbing species in emulsion systems were investigated. The TG signals from these systems show distinct features compared with that normally observed from a homogeneous solution. The DTG signal from an O/W emulsion shows a rapid rise within the excitation pulse width, and decays within 30 ns. A DTG signal which decays with a rate constant of $2D_{th}q^2$ could not be observed. The acoustic wave from this system shows a higher frequency component. The DTG signal from the W/O emulsion consists of two rising components. One of them rises rapidly within the excitation laser pulse and the other rises rather slowly. The signal decays to the baseline single exponentially with a rate constant close to $2D_{th}q^2$.

These different features can be explained well by a droplet heating effect in the emulsions. For the O/W emulsion, after heating of the droplets, they are thermally expanded, and the density variation produces the TG signal. The thermal conduction from the droplet (xylene) to the dispersion medium (water) decreases the TG intensity because the thermal expansion coefficient of water is much smaller than that of *p*-xylene. For the W/O emulsion, the local heating of the water droplets cannot contribute to the TG signal because of the small thermal expansion coefficient, while a stronger TG signal should be observed by the thermal conduction to the dispersion medium. Therefore, the rise profile of the signal should represent the thermal conduction process from the droplet to the medium. From an analysis of the temporal profile, the diameter of the dispersed particles can be estimated, and confirmed by the dynamic light scattering method. Although most of the features of the TG signal can be understood in terms of the heterogenous structure of the systems and droplet heating, there are several observations we could not explain satisfactorily in this study, such as the exact reproduction of the acoustic signal from the O/W emulsion. The origin of this feature will be elucidated in the future.

We are indebted to Prof. Diebold for his helpful discussions, particularly concerning the interpretation of the acoustic TG signal. A part of this study was supported by a Grant-in-Aid for Scientific Research from the Ministry of Education, Science, Sports and Culture.

References

1) A. Ashkin, J. M. Dziedzic, and P. W. Smith, *Opt. Lett.*, **7**, 276 (1982).

2) J. C. Kralik, B. E. Vugmeister, and M. S. Malcuit, *Phys. Rev., A*, **A51**, 32 (1995).

3) H. J. Eichler, P. Günter, and D. W. Paul, "Laser-Induced Dynamic Gratings," Springer-Verlag, Berlin (1986).

4) M. D. Fayer, *Ann. Rev. Phys. Chem.*, **33**, 63 (1982); A. E. Siegman, *J. Opt. Soc. Am.*, **67**, 545 (1977); W. J. Tomlinson and G. D. Aumiller, *Appl. Opt.*, **14**, 1100 (1975).

5) R. J. D. Miller, in "Time Resolved Spectroscopy," ed by R. J. H. Clarck and R. E. Hester, Wiley, New York (1989).

6) J. Morais, J. Ma, and M. B. Zimmt, *J. Phys. Chem.*, **95**, 3885 (1991); D. J. McGraw and J. M. Harris, *J. Opt. Soc. Am.*, **B2**, 1471 (1985); X. R. Zhu and J. M. Harris, *J. Phys. Chem.*, **93**, 75 (1989); A. Henseler and E. Vauthey, *J. Photochem. Phtobiol.* A, *Chem.*, **91**, 7 (1995); E. Vauthey and A. Henseler, *J. Phys. Chem.*, **99**, 8652 (1995).

7) M. Terazima and N. Hirota, *Chem. Phys. Lett.*, **189**, 560 (1992); M. Terazima and N. Hirota, *J. Appl. Phys.*, **73**,7672 (1993); M. Terazima and N. Hirota, *J. Chem. Phys.*, **95**, 6490 (1991).

8) K. Ohta, M. Terazima, and N. Hirota, *Bull. Chem. Soc. Jpn.*, **68**, 2809 (1995); M. Terazima, K. Okamoto, and N. Hirota, *J. Phys. Chem.*, **97**, 5188 (1993).

9) Y. Kimura, D. Kanda, M. Terazima, and N. Hirota, *Ber. Bunsenges. Phys. Chem.*, **99**, 196 (1995).

10) E. J. Heilweil and R. M. Hochstrasser, *J. Chem. Phys.*, **82**, 4762 (1985).

11) K. J. McEwan and P. A. Madden, *J. Phys. Chem.*, **97**, 8748 (1992).

12) J.-C. Bacri, A. Cebers, A. Bourdon, G. Demouchy, B. M. Heegaard, B. Kashevsky, and R. Perzynski, *Phys. Rev. E*, **52**, 3936 (1995).

13) Y. N. Cao, H. X. Chen, T. Sun, G. J. Diebold, and M. B. Zimmt, *J. Phys.*, **IV Colloque**, **C7**, 713 (1994); *Phys. Chem. B*, **101**, 3005 (1997).
14) R. A. Day, B. H. Robinson, J. H. R. Clarke, and J. V. Doherty, *J. Chem. Soc., Faraday Trans. 1*, **75**, 132 (1979).
15) J. C. Maxwell, "A Treatise on Electricity and Magnetism," 3rd ed, Dover, New York (1954), Vol. I, Chap. 9.
16) P. B. L. Chaurasia, D. R. Chaudhary, and R. C. Bhandari, *J. Appl. Chem. Biotechnol.*, **24**, 437 (1974).
17) P. B. L. Chaurasia, D. R. Chaudhary, and R. C. Bhandari, *J. Appl. Chem. Biotechnol.*, **25**, 881 (1975).
18) M. R. Wasielewski and L. D. Kispert, *Chem. Phys. Lett.*, **128**, 238 (1986); H. Hashimoto, Y. Koyama, Y. Hirata, and N. Mataga, *J. Phys. Chem.*, **95**, 3072 (1991).
19) G. M. Bilmes, J. O. Tocho, and S. E. Braslavsky, *Chem. Phys. Lett.*, **134**, 335 (1987).
20) S. E. Braslavsky and G. E. Heibel, *Chem. Rev.*, **92**, 1381 (1992).
21) Landolt–Börnstein, "Zahlenwerte und Funktionen aus Physik, Chemie, Astronomie, Geophysik und Technik," 6 Aufl., II Band, 1 Teil, S. Springer-Verlag (1971).
22) R. C. Weast, "CRC Handbook of Chemistry and Physics," 68th ed, CRC Press, Inc., Boca Raton (1987).
23) H. S. Carslaw and J. C. Jaeger, "Conduction of Heat in Solids," 2nd ed, Clarendon Press, Oxford (1959).
24) J. Crank, "The Mathematics of Diffusion," 2nd ed, Clarendon Press, Oxford (1975).
25) K. A. Nelson and M. D. Fayer, *J. Chem. Phys.*, **72**, 5202 (1980).
26) H. Chen and G. Diebold, *Science*, **270**, 963 (1995).
27) H. Chen and G. Diebold, *J. Chem. Phys.*, **104**, 6730 (1996).